# The Metal−Ligand Bifunctional Catalysis: A Theoretical Study on the Ruthenium(II)-Catalyzed Hydrogen Transfer between Alcohols and Carbonyl Compounds

**Masashi Yamakawa,[†] Hisashi Ito,[‡] and Ryoji Noyori*[,‡]**

*Contribution from the Kinjo Gakuin University, Omori, Moriyama, Nagoya 463-8521, Japan, and the Department of Chemistry and Research Center for Materials Science, Nagoya University, Chikusa, Nagoya 464-8602, Japan*

*Received May 17, 1999. Revised Manuscript Received December 6, 1999*

**Abstract:** The ternary system consisting of $[RuCl_2(\eta^6\text{-benzene})]_2$, *N*-tosylethylenediamine or ethanolamine, and KOH (Ru:amine:KOH = 1:1:2 molar ratio) catalyzes reversible hydrogen transfer between alcohols and carbonyl compounds. The use of chiral amine auxiliaries effects asymmetric transformation. The theoretical calculations using methanol/formaldehyde transformation as the model indicates the operation of a novel metal−ligand bifunctional catalysis, which is contrary to currently accepted putative pathways. The results reveal that: (1) KOH is necessary for the generation of a formal 16-electron Ru complex, $Ru(NHCH_2CH_2Y)(\eta^6\text{-benzene})$ (Y = O or NH) (catalyst), from an 18-electron Ru chloride, $RuCl(NH_2CH_2CH_2Y)(\eta^6\text{-benzene})$ (precatalyst), by a Dcb elimination of HCl, and not for increasing alkoxide concentration; (2) Ru alkoxides do not intervene in transfer hydrogenation; (3) the Ru alkoxide, even if formed, serves merely as a reservoir of the 16-electron catalyst; (4) the key 18-electron Ru hydride, $RuH(NH_2CH_2CH_2Y)(\eta^6\text{-benzene})$ (reducing intermediate), is generated by dehydrogenation of methanol with coordinatively unsaturated $Ru(NHCH_2CH_2Y)(\eta^6\text{-benzene})$; (5) this process and reverse hydrogen delivery from $RuH(NH_2CH_2CH_2Y)(\eta^6\text{-benzene})$ to formaldehyde take place by a pericyclic mechanism via a six-membered transition structure; (6) neither carbonyl oxygen nor alcoholic oxygen interacts with Ru throughout the hydrogen transfer; (7) the carbonyl oxygen atom interacts with NH on Ru and the hydroxy function with the amido nitrogen via hydrogen bonding; (8) the Ru center and nitrogen ligand simultaneously participate in both forward and reverse steps of the hydrogenation transfer. The ethanolamine- and ethylenediamine-based complexes behave similarly. In the asymmetric transformation catalyzed by chiral Ru complexes, the stereochemical bias originates primarily from the chirality of the heteroatom-based five-membered chelate rings in the transition structure. The calculated mechanism explains a range of experimental observations including the ligand acceleration effect, the structural characteristics of the isolated Ru(II) complexes, the role of the NH or $NH_2$ end of auxiliaries, the effect of a strong base cocatalyst, the kinetic profile, the reactivities of hydrogen donors and acceptors, the C=O vs C=C chemoselectivity, and the origin of enantioselection. This metal−ligand bifunctional catalysis is in sharp contrast to many other metal-centered catalyses.

## Introduction

A variety of metallic compounds promote hydrogen transfer between alcohols and carbonyl compounds. Transfer hydrogenation of ketones, for example with 2-propanol, referred to as the Meerwein−Ponndorf−Verley reduction, is effected by metal alkoxides, typically aluminum 2-propoxides, as promotors (Scheme 1).[1] The reverse process, dehydrogenative oxidation of alcohols with acetone, known as the Oppenauer oxidation, is also a useful synthetic reaction.[2] Recent studies revealed that some lanthanide salts also catalyze the same type of reaction.[3] In these cases, hydrogen transfer between the donor and acceptor molecules is thought to occur via metal alkoxides through a six-membered cyclic type **1** transition state (TS) (M = metallic species).[4] The utility of transfer hydrogenation with 2-propanol is greatly enhanced by the use of certain late transition metal complex catalysts which afford high turnover numbers.[5−7] Both

**Scheme 1.** Metal-Promoted Hydrogen Transfer between Ketones and Secondary Alcohols

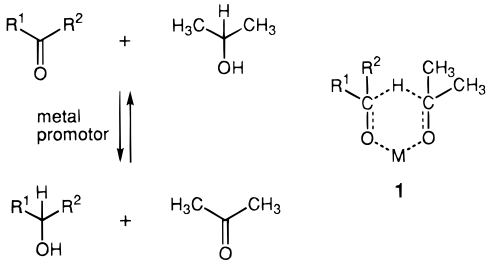


[†] Kinjo Gakuin University.

[‡] Nagoya University.

(1) Wilds, A. L. *Org. React*. **1944**, *2*, 178.

(2) (a) Djerassi, C. *Org. React*. **1951**, *6*, 207. (b) Cullis, C. F.; Fish, A. In *The Chemistry of the Carbonyl Group*; Patai, S., Ed.; Wiley: London, 1966; Vol. 1, Chapter 2.

(3) (a) Namy, J. L.; Souppe, J.; Collin, J.; Kagan, H. B. *J. Org. Chem*. **1984**, *49*, 2045. (b) Evans, D. A.; Nelson, S. G.; Gagné, M. R.; Muci, A. R. *J. Am. Chem. Soc*. **1993**, *115*, 9800.

(4) (a) Moulton, W. N.; van Atta, R. E.; Ruch, R. R. *J Org. Chem*. **1961**, *26*, 290. (b) Shiner, V. J. Jr.; Whittaker, D. *J. Am. Chem. Soc*. **1969**, 394. (c) Snyder, C. H.; Micklus, M. J. *J. Org. Chem*. **1970**, *35*, 264. (d) Casiraghi, G.; Casnati, G.; Sartori, G.; Zanafredi, G. T. *J. Chem. Soc., Perkin Trans*. **1980**, *2*, 407.

10.1021/ja991638h CCC: $19.00 
Published on Web 02/04/2000

**Scheme 2.** Transition Metal-Catalyzed Transfer Hydrogenation

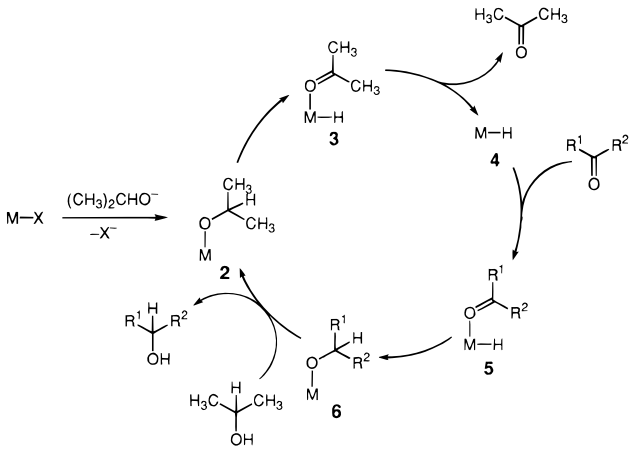

soft phosphines and hard $sp^2$-nitrogen bases have been used as standard supporting ligands.[8] Most reactions are promoted with an inorganic base such as KOH, NaOH, or $K_2CO_3$ as an essential cocatalyst.[6,7,9] Furthermore, well-designed chiral complexes containing a Ru(II),[10−17] Rh(I),[18] or Ir(I) element[19] catalyze asymmetric reduction of prochiral ketones to give chiral secondary alcohols of high enantiomeric purity.[3b,20,21] The reverse reaction can be used for kinetic resolution of racemic alcohols with acetone as the hydrogen acceptor.[12] The currently accepted putative mechanism for the standard catalytic process is outlined in Scheme 2, in which MX is a transition metal complex acting as a catalyst precursor (X = anionic ligand, typically a halide; for clarity, supporting ligands omitted).[7,21,22] This pathway involves a metal hydride intermediate, although the possibility of direct hydrogen delivery via **1** (Scheme 1) could not be eliminated.[23] The mechanism begins with displacement of X from MX by 2-propoxide to give the transition metal 2-propoxide **2**.[7,24,25] Elimination of acetone from **2**[25,26] by way of **3**[27] forms the transition metal hydride **4**.[28] Subsequently, insertion of a ketonic linkage to the M−H bond occurs via **5**,[27] resulting in the secondary alkoxide **6**.[7] Finally, ligand exchange between **6** and 2-propanol,[29] giving the alcoholic product and **2**, completes the catalytic cycle. The removal of acetone from the metal alkoxide **2**[30,31] is viewed as an analogue of the $\beta$-hydride elimination of transition metal alkyls,[32] and hence this step would require generation of a vacant cis coordination site at the metallic center.[25,33] The key issues concerning this

(5) Some early efforts: (a) Imai, H.; Nishiguchi, T.; Fukuzumi, K. *J. Org. Chem*. **1976**, *41*, 665. (b) Farnetti, E.; Vinzi, F.; Mestroni, G. *J. Mol. Catal*. **1984**, *24*, 147. (c) Smith, T. A.; Maitlis, P. M. *J. Organomet. Chem*. **1985**, *289*, 385. (d) Blum, Y.; Czarkie, D.; Rahamim, Y.; Shvo, Y. *Organometallics* **1985**, *4*, 1459. (e) Fernandez, M. J.; Esteruelas, M. A.; Covarrubias, M.; Oro, L. A. *J. Organomet. Chem*. **1986**, *316*, 343. (f) Ishii, Y.; Osakada, K.; Ikariya, T.; Saburi, M.; Yoshikawa, S. *J. Org. Chem*. **1986**, *51*, 2034. (g) Murahashi, S.-I.; Naota, T.; Ito, K.; Maeda, Y.; Taki, H. *J. Org. Chem*. **1987**, *52*, 4319. (h) Karlsson, U.; Wang, G.-Z.; Bäckvall, J.-E. *J. Org. Chem*. **1994**, *59*, 1196. (i) Wang, G.-Z. Andreasson, U.; Bäckvall, J.-E. *J. Chem. Soc., Chem. Commun*. **1994**, 1037. (j) Sheldon, R. A.; Kochi, J. K. *Metal-Catalyzed Oxidations of Organic Compounds*; Academic Press: New York, 1981.

(6) Hallman, P. S.; McGarvey, B. R.; Wilkinson, G. *J. Chem. Soc. (A)*, **1968**, 3143.

(7) (a) Bäckvall, J.-E.; Chowdhury, R. L.; Karlsson, V. *J. Chem. Soc., Chem. Commun.* **1991**, 473. (b) Wang, G.-Z.; Bäckvall, J.-E. *J. Chem. Soc., Chem. Commun*. **1992**, 337. (c) Bäckvall, J.-E.; Chowdhury, R. L.; Karlsson, U.; Wang, G.-Z. In *Perspectives in Coordination Chemistry*; Williams, A. F., Floriani, C., Merbach, A. E., Eds.; Verlag Helvetica Chimica Acta: Basel, 1992; p 463. (d) Almeida, M. L. S.; Beller, M.; Wang, G.-Z.; Bäckvall, J.-E. *Eur. J. Chem*. **1996**, *2*, 1533.

(8) For the use of $sp^3$-nitrogen bases, see: (a) Gamez, P.; Fache, F.; Mangeney, P.; Lemaire, M. *Tetrahedron Lett*. **1993**, *34*, 6897. (b) Gamez, P.; Fache, F.; Lemaire, M. *Bull. Soc. Chim. Fr*. **1994**, *131*, 600. (c) Langer, T.; Helmchen, G. *Tetrahedron Lett*. **1996**, *37*, 1381. (d) Jiang, Y.; Jiang, Q.; Zhu, G.; Zhang, X. *Tetrahedron Lett*. **1997**, *38*, 6565. (e) Touchard, F.; Gamez, P.; Fache, F.; Lemaire, M. *Tetrahedron Lett*. **1997**, *38*, 2275.

(9) For reaction without alkaline bases: Mizushima, E.; Yamaguchi, M.; Yamagishi, T. *Chem. Lett*. **1997**, 237.

(10) Hashiguchi, S.; Fujii, A.; Takehara, J.; Ikariya, T.; Noyori, R. *J. Am. Chem. Soc*. **1995**, *117*, 7562.

(11) Takehara, J.; Hashiguchi, S.; Fujii, A.; Inoue, S.-I.; Ikariya, T.; Noyori, R. *J. Chem. Soc., Chem. Commun*. **1996**, 233.

(12) Hashiguchi, S.; Fujii, A.; Haack, K.-J.; Matsumura, K.; Ikariya, T.; Noyori, R. *Angew. Chem., Int. Ed. Engl.* **1997**, *36*, 288.

(13) Haack, K.-J.; Hashiguchi, S.; Fujii, A.; Ikariya, T.; Noyori, R. *Angew. Chem., Int. Ed. Engl.* **1997**, *36*, 285.

(14) Gao, J.-X.; Ikariya, T.; Noyori, R. *Organometallics* **1996**, *15*, 1087.

(15) Noyori, R.; Hashiguchi, S. *Acc. Chem. Res*. **1997**, *30*, 97.

(16) (a) Mashima, K.; Abe, T.; Tani, K. *Chem. Lett*. **1998**, 1199. (b) Mashima, K.; Abe, T.; Tani, K. *Chem Lett*. **1998**, 1201. (c) Murata, K.; Ikariya, T.; Noyori, R. *J. Org. Chem*. **1999**, *64*, 2186.

(17) (a) Chowdhury, R. L.; J.-E. Bäckvall, *J. Chem. Soc., Chem. Commun*. **1991**, 1063. (b) Genêt, J.-P.; Ratovelomanana-Vidal, V.; Pinel, C. *Synlett* **1993**, 478. (c) Krasik, P.; Alper, H. *Tetrahedron* **1994**, *50*, 4347. (d) Jiang, Y.; Jiang, Q.; Zhu, G.; Zhang, X. *Tetrahedron Lett*. **1997**, *38*, 215. (e) Palmer, M.; Walsgrove, T.; Wills, M. *J. Org. Chem*. **1997**, *62*, 5226. (f) Alonso, D. A.; Guijarro, D.; Pinho, P.; Temme, O.; Andersson, P. G. *J. Org. Chem*. **1998**, *63*, 2749. (g) Jiang, Y.; Jiang, Q.; Zhang, X. *J. Am. Chem. Soc*. **1998**, *120*, 3817.

(18) (a) Gamez, P.; Fache, F.; Lemaire, M. *Tetrahedron: Asymmetry* **1995**, *6*, 705. (b) Yang, H.; Alvarez, M.; Lugan, N.; Mathieu, R. *J. Chem. Soc., Chem. Commun*. **1995**, 1721. (c) Jiang, Q.; Plew, D. V.; Murtuza, S.; Zhang, X. *Tetrahedron Lett*. **1996**, *37*, 797.

(19) (a) Müller, D.; Umbricht, G.; Weber, B.; Pfaltz, A. *Helv. Chim. Acta* **1991**, *74*, 232. (b) Inoue, S.-I.; Nomura, K.; Hashiguchi, S.; Noyori, R.; Izawa, Y. *Chem. Lett*. **1997**, 957.

(20) For reaction using formic acid as hydrogen donor, see: (a) Fujii, A.; Hashiguchi, S.; Uematsu, N.; Ikariya, T.; Noyori, R. *J. Am. Chem. Soc*. **1996**, *118*, 2521. (b) Uematsu, N.; Fujii, A.; Hashiguchi, S.; Ikariya, T.; Noyori, R. *J. Am. Chem. Soc*. **1996**, *118*, 4916.

(21) Reviews: (a) Zassinovich, G.; Mestroni, G. *Chem. Rev*. **1992**, *92*, 1051. (b) de Graauw, C. F.; Peters, J. A.; van Bekkum, H.; Huskens, J. *Synthesis* **1994**, 1007.

(22) (a) Tani, K.; Suwa, K.; Tanigawa, E.; Yoshida, T.; Okano, T.; Otsuka, S. *Chem. Lett*. **1982**, 261. (b) Jung, C. W.; Garrou, P. E. *Organometallics* **1982**, *1*, 658. (c) Tani, K.; Tanigawa, E.; Tatsuno, Y.; Otsuka, S. J. *Organomet. Chem*. **1985**, *279*, 87. (d) Morton, D.; Cole-Hamilton, D. J. *J. Chem. Soc., Chem. Commun*. **1987**, 248.

(23) Schröder, D.; Schwarz, H. *Angew. Chem., Int. Ed. Engl*. **1990**, *29*, 910.

(24) Bryndza, H. E.; Tam, W. *Chem. Rev*. **1988**, *88*, 1163.

(25) (a) Morton, D.; Cole-Hamilton, D. J. *J. Chem. Soc., Chem. Commun.* **1988**, 1154. (b) Blum, O.; Milstein, D. *Angew. Chem., Int. Ed. Engl*. **1995**, *34*, 229.

(26) (a) Arnold, D. P.; Bennet, M. A. *J. Organometal Chem*. **1980**, *199*, C17. (b) Osakada, K.; Ohshiro, K.; Yamamoto, A. *Organometallics* **1991**, *10*, 404.

(27) Transition metal/ketone or aldehyde complexes: (a) Green, M. L. H.; Parkin, G.; Moynihan, K. J.; Prout, K. *J. Chem. Soc., Chem. Commun*. **1984**, 1540. (b) Huang, Y.-H. Gladysz, J. A. *J. Chem. Educ*. **1988**, *65*, 298. (c) Shambayati, S.; Schreiber, S. L. In *Comprehensive Organic Synthesis*; Trost, B. M., Ed.; Pergamon: New York, 1991; Vol. 1, Chapter 1.10, p 283.

(28) (a) Sasson, Y.; Blum, J. *Tetrahedron Lett*. **1974**, 2167. (b) Sasson, Y.; Blum, J. *J. Org. Chem*. **1975**, *40*, 1887. (c) Dobson, A.; Robinson, S. D. *Inorg. Chem*. **1977**, *16*, 137. (d) Shinoda, S.; Itagaki, H.; Saito, Y. *J. Chem. Soc., Chem. Commun*. **1985**, 860. (e) Morton, D.; Cole-Hamilton, D. J.; Utuk, I. D.; Paneque-Sosa, M.; Lopez-Poveda, M. *J. Chem. Soc., Dalton Trans*. **1989**, 489. (f) Menashe, N.; Shvo, Y. *Organometallics* **1991**, *10*, 3885. (g) Fujii, T.; Saito, Y. *J. Mol. Cat*. **1991**, *67*, 185.

(29) (a) Bryndza, H. E.; Calabrese, J. C.; Marsi, M.; Roe, D. C.; Tam, W.; Bercaw, J. E. *J. Am. Chem. Soc*. **1986**, *108*, 4805. (b) Kim, Y.-J.; Osakada, K.; Takenaka, A.; Yamamoto, A. *J. Am. Chem. Soc*. **1990**, *112*, 1096.

(30) (a) Kaesz, H. D.; Saillant, R. B. *Chem. Rev*. **1972**, *72*, 231. (b) Schunn, R. A. In *Transition Metal Hydrides*; Muetterties, E. L., Ed.; Marcel Dekker: New York, 1971; pp 203−269. (c) Bryndza, H. E.; Fong, L. K.; Paciello, R. A.; Tam, W.; Bercaw, J. E. *J. Am. Chem. Soc*. **1987**, *109*, 1444. (d) Hoffman, D. M.; Lappas, D.; Wierda, D. A. *J. Am. Chem. Soc*. **1989**, *111*, 1531. (e) Blum, O.; Milstein, D. *J. Am. Chem. Soc*. **1995**, *117*, 4582.

(31) (a) Vaska, L.; DiLuzio, J. W. *J. Am. Chem. Soc*. **1962**, *84*, 4989. (b) Chatt, J.; Shaw, B. L. *J. Chem. Soc*. **1962**, 5075.

(32) (a) Thorn, D. L.; Hoffmann, R. *J. Am. Chem. Soc*. **1978**, *100*, 2079. (b) Koga, N.; Morokuma, K. *Chem. Rev*. **1991**, *91*, 823.

(33) Crabtree, R. H. *The Organometallic Chemistry of the Transition Metals, 2nd ed.*; Wiley: New York, 1994; pp 57−59 and p 223.

**Scheme 3.** Ruthenium(II)-Catalyzed Asymmetric Hydrogen Transfer Reaction

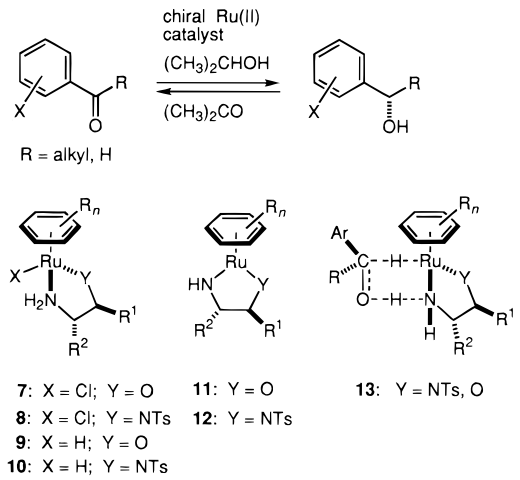


mechanism are the capability of M to carry alkoxide[7,24] and hydride ligands[34] and the Lewis acidity to accommodate ketones.[27] The role of an alkaline base is believed to involve an increase in the concentration of 2-propoxide anion[7,25] and also the deprotonation of 2-propanol coordinated to M to form **2**, thereby facilitating the overall reaction.[33] Scheme 2 is constructed by combining known stoichiometric reactions. All of the elementary steps have been well-established with model compounds and are therefore viable under catalytic conditions.

Thus, Scheme 2 reasonably explains the previously reported transfer hydrogenation catalyzed by transition metal complexes that normally possess tertiary phosphines or $sp^2$-hybridized amine ligands.[21] However, it seriously contradicts our recent findings in reaction using *primary or secondary amine ligands*.[10−15] The classical mechanism in Scheme 1 does not explain the observations either. We showed that a combined system of $[RuCl_2(\eta^6\text{-arene})]_2$ and a $\beta$-amino alcohol or N-monosulfonylated 1,2-diamine catalyzes reduction of ketones in 2-propanol containing KOH. The presence of an NH or $NH_2$ in the auxiliaries is crucial for catalytic activity; the corresponding dialkylamino analogues are totally ineffective. Sulfonyl functionality in the 1,2-diamines simply enhances acidity of the remaining NH proton to stabilize the five-membered chelate Ru(II) complexes in 2-propanol. 1,2-Diamines and 1,2-diols are ineffective. Most notable is the asymmetric catalysis given in Scheme 3. The octahedral complex **8**, with a well-shaped chiral ancillary (for example, arene = *p*-cymene and mesitylene, $R^1 = R^2 = C_6H_5$) effects the enantioselective reactions of various achiral ketones in 2-propanol containing KOH at a 200:1 substrate/catalyst molar ratio at room temperature, leading to the corresponding secondary alcohols in up to 97% ee.[10] The precatalyst **8**, true catalyst **12**, and intermediate **10** have been characterized by X-ray crystallography.[13] A kinetic study with the isolated complexes showed that, in the steady-state acetone/2-propanol catalytic cycle, the interconversion between **10** and **12** (arene = *p*-cymene; $R^1 = R^2$ = phenyl) takes place either directly or via a very short-lived intermediate and that no other complexes that limit the catalytic turnover are involved.[13] Hydrogenation of acetone with **10** and dehydrogenation of 2-propanol with **12** are equally facile. The unique 16-electron complex **12** dehydrogenates various primary and secondary alcohols, but not *tert*-butyl alcohol, to give the 18-electron Ru hydride **10** and the corresponding carbonyl compounds. The hydride **10** upon exposure to acetone reverts back to the original didehydro complex **12**.[35] Hydrogen transfer in the presence of **10** or **12** occurs even in the absence of KOH. Replacement of *N*-tosyl-1,2-diamines by $\beta$-amino alcohols effects the reaction equally,[11] indicating the involvement of analogous Ru complexes **7**, **9**, and **11** in the catalytic process. Various chiral amino alcohols can be used for asymmetric reduction of aromatic ketones. These observations are in accord with a mechanism involving the cyclic TS **13** in the hydrogen transfer reaction.

Such intriguing findings prompted us to investigate the cource of the reaction and the structural characteristics of the Ru complexes by theoretical calculations.[36] The theoretical study described below necessitates a drastic change in the putative mechanism given in Scheme 2, and supports a new metal−ligand bifunctional mechanism involving TS type **13**.[11,37]

## Results

Molecular orbital (MO) calculations were performed largely by using a model hydrogen transfer reaction between methanol and formaldehyde. When necessary, larger alcohols and carbonyl compounds were also used. Density functional theory (DFT)-based calculation was also made on certain important subjects. The Ru complex **14** is formed from $RuCl_2(\eta^6\text{-benzene})$ dimer, ethanolamine or ethylenediamine (a simplified form of the *N*-tosyl derivative), and KOH in a 1:1:2 molar ratio with Ru complex considered as a monomer. The Gaussian series programs[38] were used for all calculations. All geometries of TSs as well as those of equilibrium structures were fully optimized by the frozen-core second-order Møller−Plesset perturbation (MP2) method using the basis set of 8 valence-electron effective core potentials (ECP) of Hay and Wadt with the [3s3p3d]/(3s3p4d) basis functions[39] for Ru and the 6-31G(d) basis set for H, C, N, and O (MP2/BS-I). All of the TSs were optimized with a Hessian matrix possessing a negative eigen value. These structures were relaxed after giving a small perturbation to ensure that they were connected to the corresponding reactants and products. A vibrational analysis was performed for the two important TSs, **17a** and **20a**, to confirm that they have only one imaginary frequency. MP4(SDQ) single-point energy calculations were performed for all of the TSs and intermediates of the MP2-optimized geometry using a basis set of 16 valence-electron ECP of Hay and Wadt with the [5s3p3d]/(5s5p4d) basis functions[40] for Ru, the 6-31++G(d,p) basis set for Ru−*H*, OC−*H*, NC−*H*, $CH_3CH_2$−*H*, and H−*H*, and the 6-31G(d) basis set for other H, C, N, and O (BS-II). The Mulliken charge was

(34) (a) Jessop, P. G.; Morris, R. H. *Coord. Chem. Rev.* **1992**, *121*, 155. (b) Heinekey, D. M.; Oldham, W. J., Jr. *Chem. Rev.* **1993**, *93*, 913.

(35) Review on platinum metal amides: Fryzuk, M. D.; Montgomery, C. D. *Coord. Chem. Rev.* **1989**, *95*, 1.

(36) For previous theoretical studies on hydrogen transfer using 2-propanol, see: Itagaki, H.; Koga, N.; Morokuma, K.; Saito, Y. *Organometallics* **1993**, *12*, 1648.

(37) See structure **34** in ref 15.

(38) Frisch, M. J.; Trucks, G. W.; Schlegel, H. B.; Scuseria, G. E. Robb, M. A.; Cheeseman, J. R.; Zakrzewski, V. G.; Montgomery, J. A. Jr.; Stratmann, R. E.; Burant, J. C.; Dapprich, S.; Millam, J. M.; Daniels, A. D.; Kudin, K. N.; Strain, M. C.; Farkas, O.; Tomasi, J.; Barone, V.; Cossi, M.; Cammi, R.; Mennucci, B.; Pomelli, C.; Adamo, C.; Clifford, S.; Ochterski, J.; Petersson, G. A.; Ayala, P. Y.; Cui, Q.; Morokuma, K.; Malick, D. K.; Rabuck, A. D.; Raghavachari, K.; Foresman, J. B.; Cioslowski, J.; Ortiz, J. V.; Stefanov, B. B.; Liu, G.; Liashenko, A.; Piskorz, P.; Komaromi, I.; Gomperts, R.; Martin, R. L.; Fox, D. J.; Keith, T.; Al-Laham, M. A.; Peng, C. Y.; Nanayakkara, A.; Gonzalez, C.; Challacombe, M.; Gill, P. M. W.; Johnson, B.; Chen, W.; Wong, M. W.; Andres, J. L.; Gonzalez, C.; Head-Gordon, M.; Replogle, E. S.; Pople, J. A. *Gaussian 98*, revision A.6; Gaussian, Inc.: Pittsburgh, PA, 1998.

(39) Hay, P. J.; Wadt, W. R. *J. Chem. Phys.* **1985**, *82*, 270.

(40) Hay, P. J.; Wadt, W. R. *J. Chem. Phys.* **1985**, *82*, 299.

**Scheme 4.** Calculated Mechanism for Ruthenium(II)-Catalyzed Hydrogen Transfer between Methanol and Formaldehyde. Relative Energies Calculated at B3LYP/BS-V//B3LYP/BS-III in Parentheses

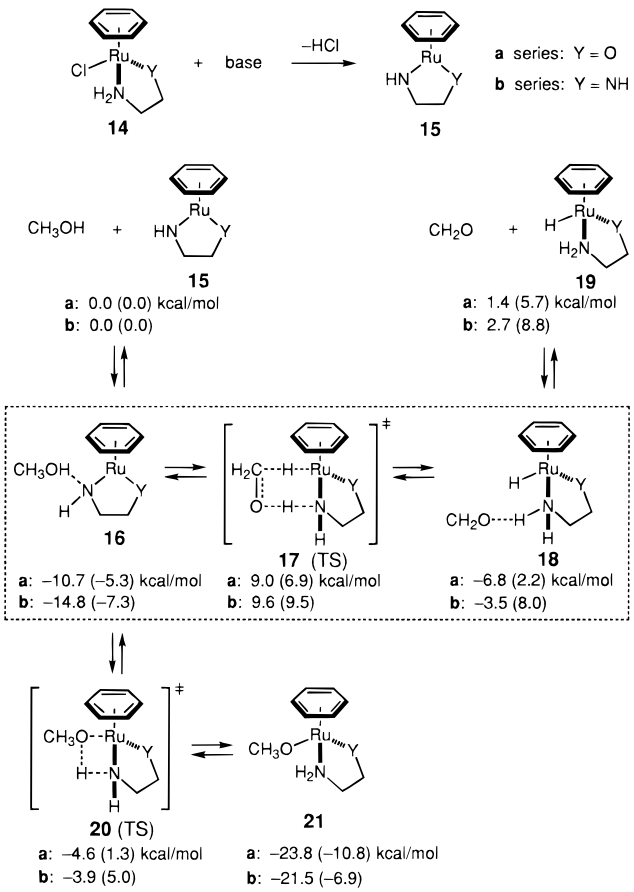


determined from the MO calculations obtained by the HF/BS-I procedure.

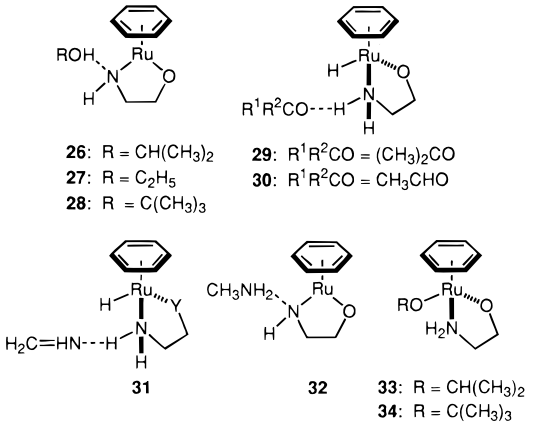


Scheme 4 illustrates the complexes present in the reaction system and their detailed three-dimensional structures are given in Figure 1. The energies are summarized in Table 1. The calculated catalytic pathway is remarkably simple as shown in the box in Scheme 4. This novel metal−ligand bifunctional mechanism involves only two ground-state compounds, **16** and **18**. Transition structures of hydrogen transfer are summarized in Figure 2. Figure 3 illustrates the energy correlation diagram of the reaction. Other structures are given in Supporting Information.

Unless otherwise stated, the argument is based mainly on the MO calculations. To verify these calculations, however, the geometries of the important intermediates and transition states have also been optimized using Becke's three-parameter hybrid functioanal method (B3LYP).[41] Relativistic 16 valence-electron effective core potentials[40] with the valence split basis functions (LANL2DZ) were used for Ru, and the 6-31G(d,p) basis sets were employed for other atoms (BS-III). Vibrational frequencies and zero-point energies (ZPE) have also been calculated at the B3LYP/BS-III level. The structures reported here are either

**Table 1.** Relative Energies (kcal/mol) of Intermediates and Transition States in Hydrogen Transfer Catalyzed by Ruthenium(II) Complexes

| compound | MP2/BS-I// MP2/BS-I | MP4(SDQ)/ BS-II//MP2/BS-I |
|---|---|---|
| Interconversion of $CH_3OH$ and $CH_2O$ (**a** series) | | |
| $CH_3OH$ + **15a** | 0.0 | 0.0 |
| **16a** | −11.8 | −10.7 |
| **17a** (TS) | 8.8 | 9.0 |
| ***anti*-17a** (TS) | 12.7 | 13.2 |
| **18a** | −1.1 | −6.8 |
| $CH_2O$ + **19a** | 7.3 | 1.4 |
| $CH_2O$ + ***anti*-19a** | 10.5 | 4.9 |
| **20a** (TS) | −8.9 | −4.6 |
| **21a** | −25.3 | −23.8 |
| ***anti*-21a** | −20.8 | −19.1 |
| **22** | 10.7 | 9.9 |
| **23** (TS) | 12.2 | 12.7 |
| **24** | −1.0 | 3.3 |
| **25** (TS) | 19.3 | 17.3 |
| Interconversion of $CH_3OH$ and $CH_2O$ (**b** series) | | |
| $CH_3OH$ + **15b** | 0.0 | 0.0 |
| **16b** | −16.1 | −14.8 |
| **17b** (TS) | 9.1 | 9.6 |
| **18b** | 1.4 | −3.5 |
| $CH_2O$ + **19b** | 7.9 | 2.7 |
| **20b** (TS) | −8.2 | −3.9 |
| **21b** | −23.3 | −21.5 |
| Interconversion of $(CH_3)_2CHOH$ and $(CH_3)_2CO$ | | |
| $(CH_3)_2CHOH$ + **15a** | 0.0 | 0.0 |
| **26** | −12.5 | −11.2 |
| **35** (TS) | 5.0 | 5.4 |
| **29** | −10.5 | −16.6 |
| $(CH_3)_2CO$ + **19a** | −0.6 | −6.8 |
| Interconversion of $CH_3CH_2OH$ and $CH_3CHO$ | | |
| $CH_3CH_2OH$ + **15a** | 0.0 | 0.0 |
| **27** | −12.2 | −11.0 |
| $\mathbf{36}_S$ (TS) | 6.0 | 6.2 |
| $\mathbf{36}_R$ (TS) | 6.4 | 6.8 |
| **30** | −7.0 | −12.7 |
| $CH_3CHO$ + **19a** | 2.1 | −3.8 |
| Heterolysis of $H_2$ | | |
| $H_2$ + **15a** | 0.0 | 0.0 |
| **37** (TS) | 27.0 | 25.2 |
| **19a** | −14.2 | −20.9 |
| Conversion of $CH_2$═NH to $CH_3NH_2$ | | |
| $CH_2$═NH + **19a** | 0.0 | 0.0 |
| **31** | −9.8 | −9.3 |
| **38** (TS) | 9.8 | 17.6 |
| **32** | −23.8 | −16.3 |
| $CH_3NH_2$ + **15a** | −15.7 | −8.8 |
| Conversion of $CH_2$═$CH_2$ to $CH_3CH_3$ | | |
| $CH_2$═$CH_2$ + **19a** | 0.0 | 0.0 |
| **39** (TS) | 18.0 | 26.7 |
| $CH_3CH_3$ + **15a** | −27.1 | −19.6 |
| Addition of $(CH_3)_2CHOH$ to **15a** | | |
| $(CH_3)_2CHOH$ + **15a** | 0.0 | 0.0 |
| **26** | −12.5 | −11.2 |
| **33** | −25.9 | −24.5 |
| Addition of $(CH_3)_3COH$ to **15a** | | |
| $(CH_3)_3COH$ + **15a** | 0.0 | 0.0 |
| **28** | −13.2 | −12.7 |
| **34** | −22.7 | −22.0 |

(41) (a) Becke, A. D. *J. Chem. Phys.* **1993**, *98*, 5648. (b) Lee, C.; Yang, W.; Parr, R. G. *Phys. Rev.* **1988**, *B37*, 785.

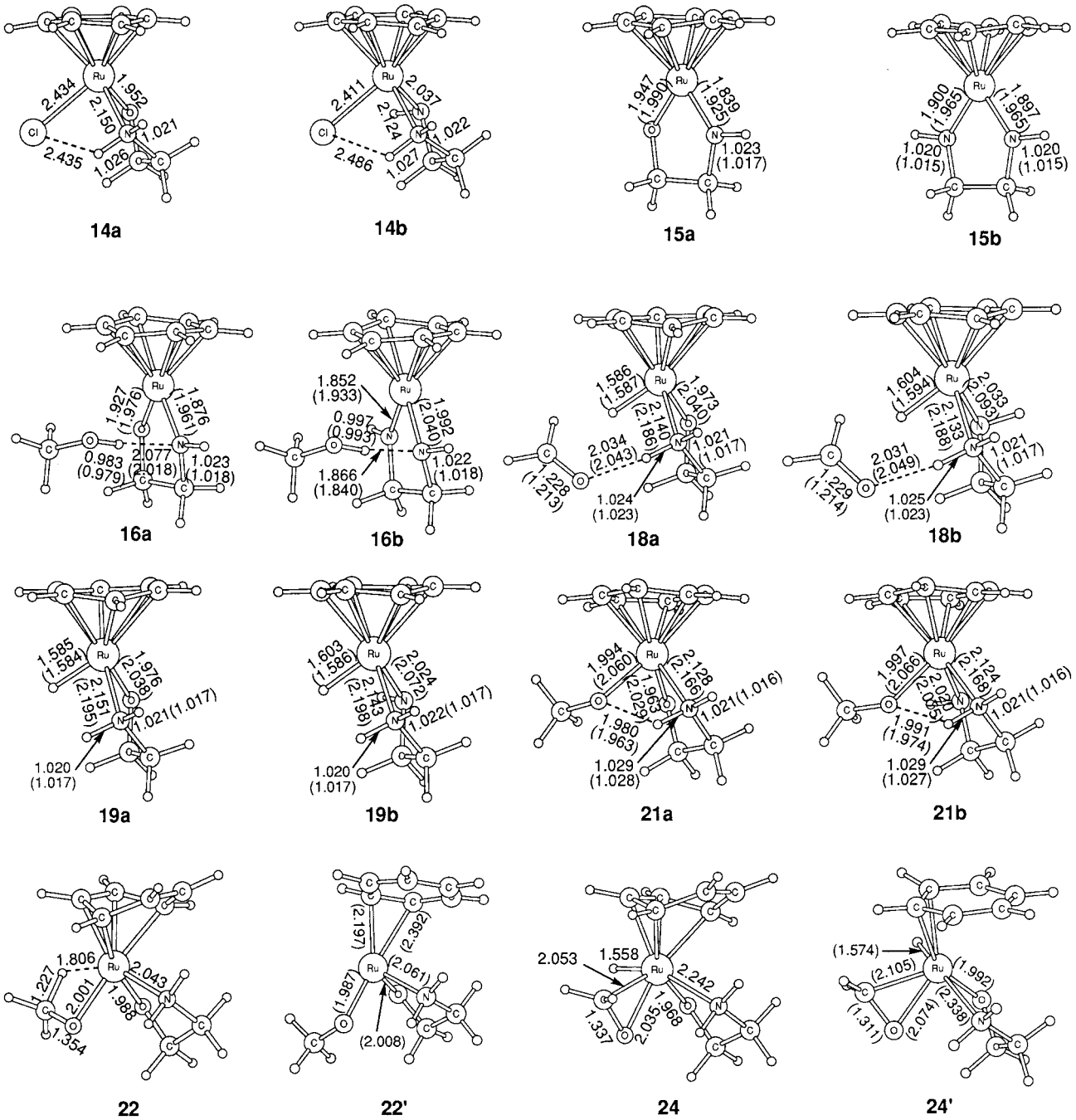


**Figure 1.** Structures of ruthenium(II) complexes optimized at the MP2/BS-I level. Bond lengths of the complexes optimized at the B3LYP/BS-III level are given in parentheses.

minima (number of imaginary frequency = 0) or transition states (number of imaginary frequency = 1) on the potential-energy surface. The ZPE correction are unscaled. Improved total energies were calculated at the B3LYP level using the same ECP and valence basis set for Ru, but contracted to triple-$\zeta$ and augmented with one set of f-type polarization functions ($\zeta$ = 1.235)[42] together with 6-311G(d,p) basis sets for other atoms (BS-IV). The total energies were further improved by using BS-IV after changing the 6-311G(d,p) basis set for H, C, N, and O (except for the benzene ligand) to the 6-311++G(d,p) basis set (BS-V). The calculated relative energies are shown in Table 2, and the structural parameters are given in parentheses in Figures 1 and 2. Other structures are given in Supporting Information.

**(a) Structures of Ru(II) Catalysts.** The Ru(II)-catalyzed reaction aided by ethanolamine[11] starts from the precatalyst **14a** possessing a distorted octahedral geometry. The five-membered chelate ring is highly skewed and has two diastereotopic nitrogen-bound hydrogens, $H_{ax}$ (axial) and $H_{eq}$ (equatorial). The $NH_{ax}\cdots Cl$ distance, 2.435 Å, is much shorter than the sum of the van der Waals distance, 3.0 Å, suggesting the existence of hydrogen bond attraction. In fact, the $N-H_{ax}$ bond is 0.5% longer than the $N-H_{eq}$ bond, 1.026 vs 1.021 Å.

The base-promoted elimination of HCl from **14a** forms the true catalyst **15a** with a 16-electron configuration. Without base, this process is endothermic by 36.5 kcal/mol. The square-planar structure **15a** possesses a hexagonal benzene ring and an anionic

(42) Ehlers, A. W.; Böhme, M.; Dapprich, S.; Gobbi, A.; höllwarth, A.; Jonas, V.; Köhler, K. F.; Stegmann, R.; Veldkamp, A.; Frenking, G. *Chem. Phys. Lett.* **1993**, *208*, 111.

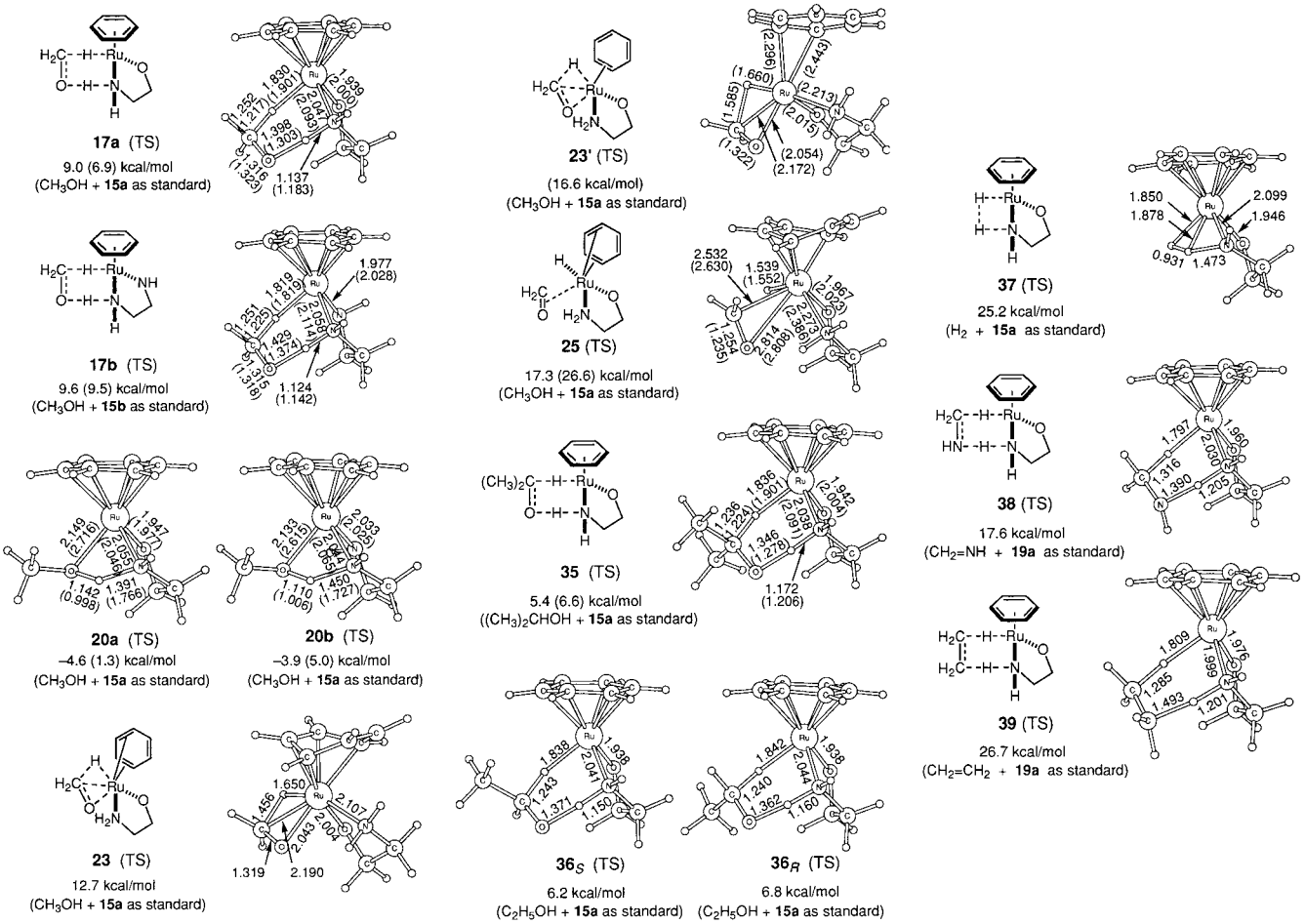


**Figure 2.** Transition structures of hydrogen transfer optimized at the MP2/BS-I level. Bond lengths and relative energies calculated at the B3LYP/BS-III level are given in parentheses.

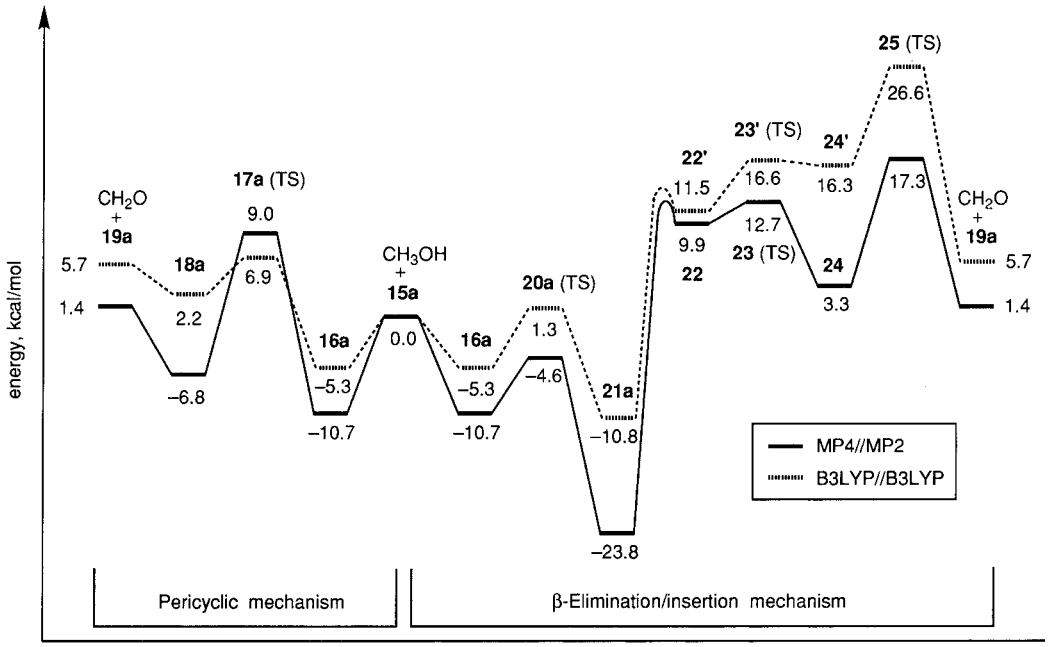


**Figure 3.** Energy diagram for pericyclic mechanism (left) and $\beta$-elimination/insertion mechanism (right) obtained at the MP4/BS-II//MP2/BS-I and B3LYP/BS-V//B3LYP/BS-III levels.

nitrogen and oxygen ligand.[24,35,44] The benzene ligand, placed perpendicular to the N−Ru−O plane, acts as a bis-3-electron donor (neutral formalism),[45] in which the C(6)−C(1) and C(3)−C(4) distances, 1.44 (1.44) Å,[43] are slightly longer than other C−C bonds, 1.41−1.43 (1.41−1.42) Å. The Ru amide bond, 1.839 (1.925) Å, is much shorter than the normal Ru−N distance, 2.16 Å.[46] The nitrogen has a planar geometry with a sum of the three angles of 357.5°. The Ru−O distance, 1.947 Å, is also shorter than that in **14a**, 1.952 Å. Thus, the electron deficiency of the Ru center is mitigated by substantial electron

**Table 2.** Relative Energies (kcal/mol) of Some Important Intermediates and Transition States in Hydrogen Transfer Catalyzed by Ruthenium(II) Complexes Calculated at the B3LYP Level

| compound | B3LYP/BS-III// B3LYP/BS-III uncorrected | B3LYP/BS-III// B3LYP/BS-III ZPE[a] | B3LYP/BS-IV// B3LYP/BS-III[b] | B3LYP/BS-V// B3LYP/BS-III[b] |
|---|---|---|---|---|
| Interconversion of $CH_3OH$ and $CH_2O$ (**a** series) | | | | |
| $CH_3OH$ + **15a** | 0.0 | 0.0 | 0.0 | 0.0 |
| **16a** | −9.1 | 1.3 | −7.6 | −5.3 |
| **17a** (TS) | 5.2 | −1.7 | 6.1 | 6.9 |
| **18a** | −1.6 | −0.8 | −0.8 | 2.2 |
| $CH_2O$ + **19a** | 5.3 | −2.2 | 4.0 | 5.7 |
| **20a** (TS) | −5.0 | 1.4 | −1.7 | 1.3 |
| **21a** | −17.8 | 2.5 | −14.3 | −10.8 |
| **22′** | 1.2 | 1.9 | 7.8 | 11.5 |
| **23′** (TS) | 9.5 | −0.4 | 13.1 | 16.6 |
| **24′** | 8.3 | 0.5 | 12.6 | 16.3 |
| **25** (TS) | 22.4 | −0.9 | 23.7 | 26.6 |
| Interconversion of $CH_3OH$ and $CH_2O$ (**b** series) | | | | |
| $CH_3OH$ + **15b** | 0.0 | 0.0 | 0.0 | 0.0 |
| **16b** | −12.3 | 1.7 | −10.1 | −7.3 |
| **17b** (TS) | 6.6 | −1.0 | 8.8 | 9.5 |
| **18b** | 3.3 | −0.5 | 5.1 | 8.0 |
| $CH_2O$ + **19b** | 7.3 | −1.8 | 7.1 | 8.8 |
| **20b** (TS) | −1.0 | 1.3 | 2.6 | 5.0 |
| **21b** | −15.1 | 2.6 | −10.7 | −6.9 |
| Interconversion of $(CH_3)_2CHOH$ and $(CH_3)_2CO$ | | | | |
| $(CH_3)_2CHOH$ + **15a** | 0.0 | 0.0 | 0.0 | 0.0 |
| **26** | −8.8 | 1.1 | −7.2 | −4.7 |
| **35** (TS) | 5.2 | −2.5 | 5.8 | 6.6 |
| **29** | −12.4 | −1.1 | −11.5 | −9.3 |
| $(CH_3)_2CO$ + **19a** | −5.0 | −2.0 | −5.7 | −4.6 |
| Addition of $(CH_3)_2CHOH$ to **15a** | | | | |
| $(CH_3)_2CHOH$ + **15a** | 0.0 | 0.0 | 0.0 | 0.0 |
| **26** | −8.8 | 1.1 | −7.2 | −4.7 |
| **33** | −16.1 | 2.2 | −12.2 | −9.0 |

[a] Zero-point energy. [b] Corrected with zero-point energy.

donation from the nonbonding orbitals of the nitrogen and oxygen as well as the bis-allylic benzene ligand. As such, the formal 16-electron complex **15a** is much more stable than it appears to be.[47]

The catalytic complex **15a** dehydrogenates methanol to give formaldehyde and **19a** with an endothermicity of 1.4 (5.7) kcal/mol.[43] The Ru hydride **19a** is an 18-electron complex with a distorted octahedral coordination sphere. The Ru−H bond has a typical length of 1.585 Å.[48] The amide ligand in **15a** now becomes a neutral amine ligand. The coordinative saturation at the Ru center substantially elongates the Ru−N bond, 2.151 (2.195) Å. The Ru−O linkage, 1.976 (2.038) Å, is also much longer than in **15a** and close to that in **14a**. The benzene ring acts as a tridentate ligand. The Ru−H bond is syn to the neighboring $N-H_{ax}$ bond. The distance between the hydrogens on Ru and N, 2.312 (2.355) Å, is relatively short (van der Waals separation, 2.4 Å) but, unlike in **14a**, the lengths of $N-H_{ax}$ and $N-H_{eq}$ are similar, 1.020 and 1.021 (1.017 and 1.017) Å.[49]

Hydrogen transfer from **19a** to formaldehyde, giving methanol and **15a**, is exothermic by 1.4 kcal/mol. The MO and DFT calculations give similar results.

**(b) Reaction Pathway of Hydrogen Transfer.** The dehydrogenation of methanol with **15a** proceeds by way of complex **16a** (Scheme 4). This initial hydrogen-bonded structure is more stable than $CH_3OH$ + **15a** by 10.7 (5.3) kcal/mol.[43] The product is **18a** which is 8.2 (3.5) kca1/mol more stable than free $CH_2O$ and **19a**, owing to the presence of an $O\cdots H_{ax}-N$ hydrogen-bond interaction. The calculation suggests that the TS **17a** is located 19.7 (12.2) kcal/mol above **16a**. In this six-membered pericyclic TS, the α hydrogen and hydroxy hydrogen of methanol have interactions with the Ru center and the amide nitrogen, respectively. Optimization of **17a** through structural peturbation resulted in **16a** or **18a**.

As a consequence of microscopic reversibility, reduction of formaldehyde, **18a** → **16a**, occurs via the same TS **17a**. The activation energy of the hydrogenation, 15.8 (4.7) kcal/mol, is lower than the value for methanol dehydrogenation in **16a**, 19.7 (12.2) kcal/mol. Note, however, that the occurrence of this pathway would be less frequent than expected from the activation energy. The geometry of **18a** with the Ru−H bond coplanar to the C═O plane (Figure 1) is much different from **17a**. The hydride transfer to the carbonyl carbon requires significant structural change. The reaction may also take place to some extent by direct bimolecular reaction between $CH_2O$ and **19a** with an activation energy of 7.6 (1.2) kcal/mol. In any case, the reaction is viewed as a nucleophilic reaction of the hydride Ru with the carbonyl carbon assisted by the $O\cdots H_{ax}-N$ hydrogen bond. Although the MO and DFT calculations give similar results, the energy barriers obtained by DFT are lower,

(43) The values in parentheses have been obtained by B3LYP.

(44) (a) Annilo, A.; Barrio, C.; García-Granda, S.; Obeso-Rosete, R. *J. Chem. Soc., Dalton Trans*. **1993**, 1125. (b) Bickford, C. C.; Johnson, T. J.; Davidson, E. R.; Caulton, K. G. *Inorg. Chem*. **1994**, *33*, 1080.

(45) (a) Silverthorn, W. E. *Adv. Organomet. Chem*. **1975**, *13*, 47. (b) Muetterties, E. L.; Bleeke, J. R.; Wucherer, E. J.; Albright, T. A. *Chem. Rev*. **1982**, *82*, 499.

(46) (a) Hartwig, J. F.; Anderson, R. A.; Bergman, R. G. *Organometallics* **1991**, *10*, 1875. (b) Burn, M. J.; Fickes, M. G.; Hollander, F. J.; Bergman, R. G. *Organometallics* **1995**, *14*, 137.

(47) Caulton, K. G. *New J. Chem*. **1994**, *18*, 25.

(48) Brammer, L.; Klooster, W. T.; Lemke, F. R. *Organometallics* **1996**, *15*, 1721.

(49) Shubina, E. S.; Belkova, N. V.; Krylov, A. N.; Vorontsov, E. V.; Epstein, L. M.; Gusev, D. G.; Niedermann, M.; Berke, H. *J. Am. Chem. Soc*. **1996**, *118*, 1105.

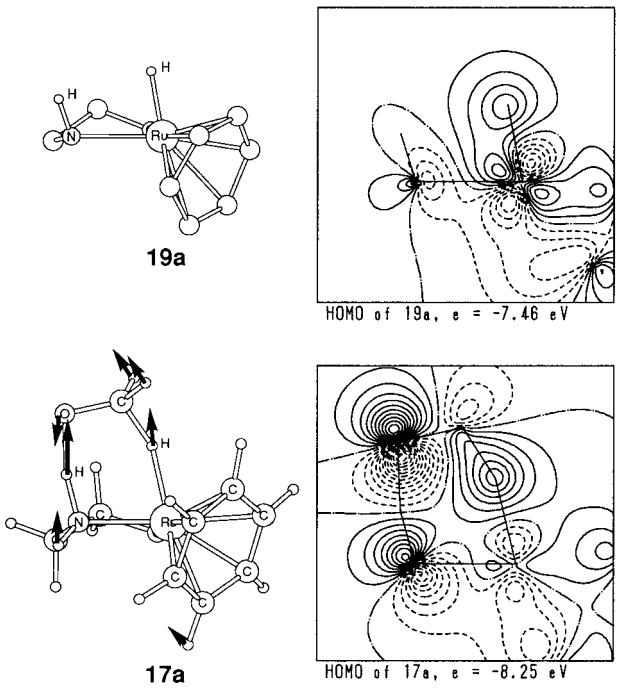


**Figure 4.** Vibration vector of 538*i* $cm^{-1}$ in transition state **17a** and contour maps of HOMOs for **17a** and **19a** in the plane that involves reacting atoms (H, Ru, N, $H_{ax}$, O, and C). Contours are separated by 0.02 $e^{1/2}$ $bohr^{-3/2}$. The solid and dashed lines indicate opposite sign.

in both forward and backward hydrogen-tranfer processes, than those of the MO calculation.

Thus, the Ru complexes **16a** and **18a** are only ground-state complexes present in this redox reaction. The TS **17a** was proven to have a single imaginary frequency of 538i $cm^{-1}$. Figure 4 illustrates the contour maps of the HOMO of **17a** and **19a**. The frequency analysis of the hydrogenation TS given in the figure indicates that the amplitude is largest at N−$H_{ax}$ and second largest at Ru−H and that the cleavage of these bonds, viz., the migration of the two hydrogen atoms to **15a** (and its reverse process) occurs synchronously. In addition, the carbonyl carbon is considerably pyramidized, and the nitrogen atom is becoming planar. As displayed in Figure 4, the HOMO of TS **17a** is strongly correlated with the HOMO of **19a** and the LUMO of $CH_2O$. The s orbital of the electrodonative hydride has bonding interaction with the vacant p orbital of carbonyl carbon, while the H−Ru bond possesses an antibonding nature. On the other hand, the N···H···O region with a node at the hydrogen atom shows a typical HOMO shape for hydrogen bonded species. The TS resembles the hydride **19a** but is different from the 16-electron complex **15a** from both MO and structural points of view. As visualized in Figures 1 and 2, the five-membered ring structure and the location of the arene ligand in **17a** and **19a** are very similar. The Ru−H length, 1.830 (1.901) Å,[43] and the N−$H_{ax}$ distance, 1.137 (1.183) Å, in **17a** are 15% (20%) and 11% (16%) longer than those of **19a** which are 1.585 (1.584) and 1.020 (1.017) Å, respectively. The C−O bond, 1.316 (1.323) Å, in **17a** is 8% (10%) longer than C═O bond of formaldehyde, 1.222 (1.207) Å, and 8% (7%) shorter than the methanol bond, 1.425 (1.418) Å, while the α-C−H bond, 1.252 (1.217) Å, and the O−H bond, 1.398 (1.303) Å, are 14% (11%) and 44% (35%) stretched from those of ground-state methanol which are 1.097 (1.101) and 0.970 (0.965) Å, respectively. The structural characteristics are not much affected by the calculation method, either MO or DFT.

The metallic center and the nitrogen ligand in the 16-electron Ru complexes cooperate in causing hydrogen transfer between

**Scheme 5.** Calculated β-Elimination Mechanism. Relative Energies Calculated at B3LYP/BS-V//B3LYP/BS-III in Parentheses

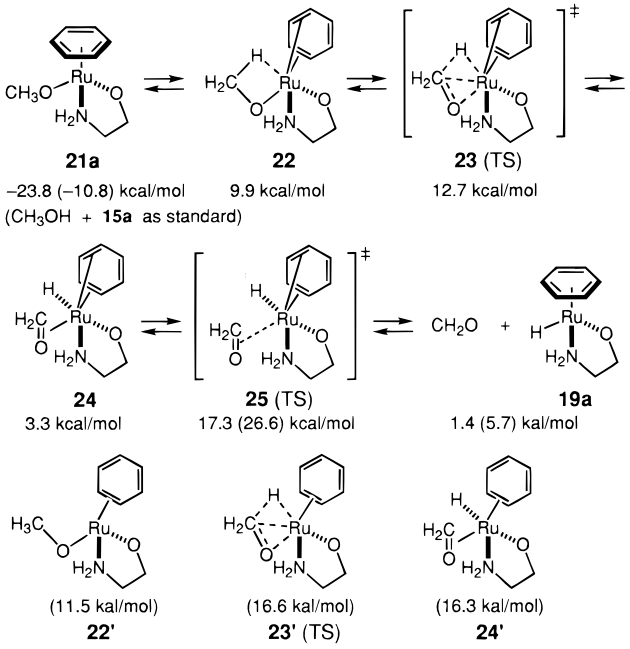


methanol and formaldehyde via TS **17a**, effecting the metal−ligand bifunctional catalysis. The high dehydrogenative activity of **15a** relies heavily on the polarized Ru−N bond, as indicated by the Mulliken charges of +1.13 at Ru and −0.72 at N. On the other hand, the hydrogenative reactivity of the 18-electron complex **19a** originates from the charge-alternating H−Ru−N−H arrangement, where the Mulliken charges are −0.05 (H), +0.69 (Ru), −1.02 (N), and +0.41 ($H_{ax}$). Thus, the key complex **19a** acts as a 1,4-dipole. The hydride on Ru possesses nucleophilicity, while the $NH_{ax}$ moiety exhibits a unique hydrogen-bonding ability to activate the carbonyl substrate. The pericyclic TS is also charge-alternated; the atomic charges of the migrating hydrogens at Ru and N are −0.19 and +0.55, respectively.

**(c) Nonproductive Reactions.** A major nonproductive process in this catalytic system is methanol addition to the 16-electron complex **15a** giving **21a**. The hydrogen-bonded complex **16a** is converted to the 18-electron methoxy complex **21a** via TS **20a** with an activation energy of only 6.1 (6.6) kcal/mol.[43] The TS **20a** has a single imaginary frequency of 781*i* $cm^{-1}$. The overall process from free $CH_3OH$ and **15a** is highly exothermic, $\Delta E = -23.8$ (−10.8) kcal/mol. The methoxy compound **21a** is stabilized by an intramolecular O···$H_{ax}$−N hydrogen bond, 1.980 (1.963) Å. The reverse process, **21a** → **16a**, requires an activation energy of 19.2 (12.1) kcal/mol.

2-Propanol and *tert*-butyl alcohol equally add to **15a** to give **33** and **34** with an exothermicity of 24.7 (9.0)[43] and 22.0 kcal/mol, respectively (Tables 1 and 2). The exothermicity calculated by DFT is considerably less than that obtained by the MO calculation mainly due to the lower stability of the DFT-calculated alkoxide complex.

**(d) β-Elimination from the Ru Methoxide and Its Reverse Process.** Certain alkoxy transition metal complexes are known to undergo β-elimination, giving metal hydrides and carbonyl compounds.[30] Since the methoxy Ru complex **21a** is coordinatively saturated, direct β-elimination from the octahedral complex seems unlikely. The calculation suggests Scheme 5 as the most probable mechanism for the formation of the Ru

hydride **19a** from the methoxide **21a**. However, we conclude that this process and its reverse reaction are much more difficult than the pericyclic process **16a** → **18a** or **18a** → **16a** (Scheme 4), because the highest-energy TS in this mechanism, **25**, is even 8.3 kcal/mol less stable than **17a** using the same standard.

The $\beta$-elimination process, **21a** → **19a** + formaldehyde, is endothermic by 25.2 kcal/mol. This reaction starts via partial decoordination of the $\eta^6$-benzene ligand to afford first the metastable Ru species **22** having an octahedral structure with a methoxy ligand with α-H···Ru agostic interaction[50] and a $\eta^4$-benzene ligand,[45] and a bidentate $\beta$-amino alkoxide. This step is highly endothermic, $\Delta E = 33.7$ kcal/mol, while any TS could not be detected by the calculation. The complex **22** then undergoes $\beta$-elimination via TS **23** with $E_a = 2.8$ kcal/mol to give **24**, in which the aldehyde carbon is considerably pyramidized. This hydride complex is more stable than **22** by 6.6 kcal/mol but less stable than **21a** by 20.5 kcal/mol. Finally, release of formaldehyde from the $\eta^4$-benzene hydrido complex **24** affords the Ru hydride **19a** with an exothermicity of 1.9 kcal/mol. This process via TS **25** requires an $E_a$ of 14.0 kcal/mol. Thus, the most difficult step in the $\beta$-elimination mechanism is the $\eta^6$ to $\eta^4$ structural change of the arene ligand, **21a** → **22**.

The reverse process, reaction of formaldehyde and **19a** leading to **24**, involves the same transition state **25**. The partial arene displacement with formaldehyde requires an $E_a$ of 15.9 kcal/mol. This reaction occurs by bimolecular collision and hence is less feasible than expected from the $E_a$ value. The reaction via the hydrogen-bonded species **18a**, requiring an $E_a$ of 24.1 kcal/mol, is also kinetically unfavorable.

The DFT calculation gives a similar energy profile, although the intermediates and TSs tend to have an $\eta^2$-arene structure instead of the $\eta^4$ structure (Scheme 5). Thus reaction of formaldehyde and the Ru hydride **19a** forms the aldehyde/Ru $\pi$ complex **24′**. This arene $\eta^6$-to-$\eta^2$ displacement is endothermic by 10.6 kcal/mol and proceeds via TS **25** with an $E_a$ of 20.9 kcal/mol. This TS is located above the pericyclic TS **17a** by even 19.7 kcal/mol. The intermediate **24′**, if formed, undergoes intramolecular hydride transfer reaction via TS **23′** to give the Ru methoxide **22′** and finally **21a**. The methoxide **22′** is a formal 14-electron complex which, unlike **22**, contains an $\eta^2$-benzene ligand and lacks any α-H···Ru agostic inteteraction.

Overall, the formation of **21a** from methanol and **15a** is thermodynamically favorable but is unproductive. The Ru-promoted methanol/formaldehyde conversion occurs much more easily via a direct pericyclic mechanism than by the multistep, $\beta$-elimination pathway involving many discrete intermediates. In a like manner, the reverse 2 + 2 reaction of **19a** and formaldehyde is also difficult. The extent of the preference of the pericyclic mechanism over the 2 + 2 mechanism is higher with the DFT calculation than the MO calculation.

**(e) Reactivity of Hydrogen Donors and Acceptors.** The equilibrium points of hydrogen transfer between alcohols and carbonyl compounds are highly affected by the nature of the hydrogen donors and acceptors.[51] Dehydrogenation of methanol with **15a** is endothermic by 1.4 (5.7) kcal/mol.[43] The $\Delta E$ value varies by going from methanol to ethanol, −3.8 kcal/mol, and 2-propanol, −6.8 (−4.6) kcal/mol. The activation energy of dehydrogenation changes from 19.7 (12.2) to 17.2 to 16.6 (11.3) kcal/mol.

Dehydrogenation of 2-propanol with **15a** is facile on both thermodynamic and kinetic grounds. Because of the high stability of acetone, the dehydrogenation occurs with an exothermicity of 6.8 (4.6) kcal/mol.[43] The TS **35** is similar in structure to that in the dehydrogenation of methanol, but it is located somewhat earlier on reaction coordinate as judged from the longer OH···N and CH···Ru distances as well as the shorter Ru−N linkage (Figure 2). Structures $\mathbf{36_S}$ and $\mathbf{36_R}$ in Figure 2 illustrate the diastereomeric TSs of hydrogen transfer between ethanol and acetaldehyde.

Acetone reacts with **19a** via **29** with $E_a = 22.0$ (15.9) kcal/mol.[43] As expected, this value is higher than the 15.8 (4.7) and 18.9 kcal/mol required for the reaction of formaldehyde and acetaldehyde, respectively.

Molecular hydrogen undergoes heterolysis[52] with **15a** to give **19a** with an exothermicity of 20.9 kcal/mol. The reaction does not involve a Ru($\eta^2$-$H_2$) complex but occurs directly via TS **37** (Figure 2) with $E_a = 25.2$ kcal/mol. Elimination of hydrogen from **19a** is kinetically difficult, requiring $E_a = 46.1$ kcal/mol.

The Ru hydride **19a** reduces methylene imine ($CH_2$═NH) by way of **38** (Figure 2), affording methylamine and **15a** with an exothermicity of 8.8 kcal/mol. The activation energy of reaction involving the hydrogen-bonded complex **31**, 26.9 kcal/mol, is 11.1 kcal/mol higher than that for reaction of $CH_2$═O. The capability of the unsaturated substrates to accept hydrogen atoms from **19a** reflects the extent of the polarity of the double bond. Ethylene accepts two hydrogens from **19a** via **39** (Figure 2) with $E_a = 26.7$ kcal/mol. The formation of ethane and **15a** is exothermic by 19.6 kcal/mol. Thus the calculations indicate that both C═X (X = O and N) and C═C bonds are saturated by the pericyclic mechanism but that the details are different. Reduction of the polar C═X bonds involves the initial hydrogen-bonded species, while the C═C linkage is saturated by a direct bimolecular mechanism. The former process is entropically much more favorable.

**(f) Diastereomeric Structures of Ru(II) Chloride, Hydride, Methoxide, and the Transition State of Hydrogen Transfer.** The Ru centers in **14a**, **19a**, and **21a** are stereogenic. Since the amino alcohol-derived five-membered chelate ring is chiral, $\delta$ or $\lambda$, diastereomers are possible for these 18-electron Ru complexes. The conformation of the chelate ring correlates well with the absolute configuration at Ru, *R* or *S*.[53] These compounds are characterized by the syn relationship between the axial N−H bond and the Ru−Cl, −H, or $-OCH_3$ linkages (Figure 1). These complexes with the same configuration are more stable than the anti stereoisomers with by 3−5 kcal/mol regardless of the anionic ligands (Figure 5). The syn isomers of the chloride and methoxide are partly stabilized by the $NH_{ax}$ to Cl or O hydrogen bond of 2.435 and 1.980 Å length, respectively. The presence of the hydrogen bonds elongates the Ru-heteroatom linkages and N−H bonds in comparison to those of the non-hydrogen-bonded isomers (chloride, 2.435 and 1.026 Å (**14a**) vs 2.407 and 1.023 Å (***anti*-14a**); methoxide, 1.994 and 1.029 Å (**21a**) vs 1.985 and 1.024 Å (***anti*-21a**)). However, such hydrogen-bond stabilization is absent in the Ru hydride **19a**. Therefore, all the above arguments were made using the $\delta$ structures.

This situation also applies to the TS of hydrogen transfer, which is due obviously to the stereoelectronic effect. Dehydro-

(50) Koga, N.; Obara, S.; Kitaura, K.; Morokuma, K. *J. Am. Chem. Soc.* **1985**, *107*, 7109.

(51) (a) Adkins, H.; Elofson, R. M.; Rossow, A. G.; Robinson, C. C. *J. Am. Chem. Soc.* **1949**, *71*, 3622. (b) Hach, V. *J. Org. Chem.* **1973**, *38*, 293.

(52) Hydrogen molecule can be cleaved in a heterolytic fashion by transition metal amide complexes. See: Fryzuk, M. D.; MacNeil, P. A.; Rettig, S. J. *J. Am. Chem. Soc.* **1987**, *109*, 2803.

(53) For the notation of the absolute configuration, see: (a) Lecomte, C.; Dusausoy, Y.; Protas, J.; Tirouflet, J.; Dormond, A. *J. Organomet. Chem.* **1974**, *73*, 67. (b) Stanley, K.; Baird, M. C. *J. Am. Chem. Soc.* **1975**, *97*, 6598.

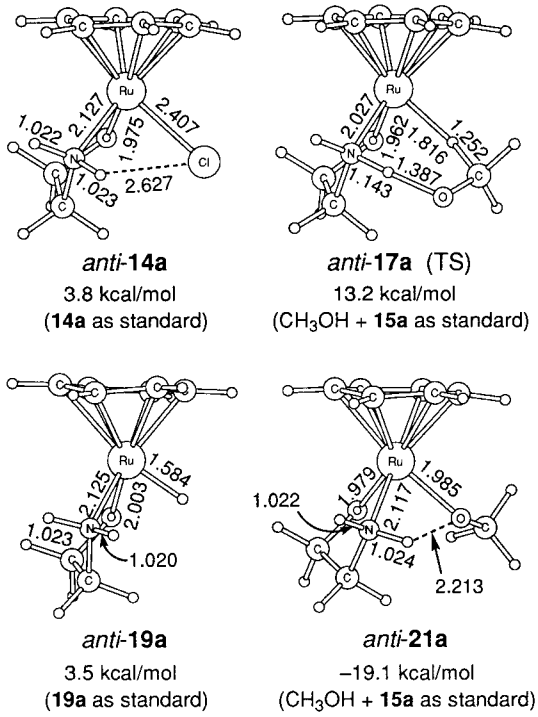


**Figure 5.** Structures of the (*R*)-$\lambda$-Ru chloride, (*R*)-$\lambda$-Ru hydride, (*R*)-$\lambda$-Ru methoxide, and related transition states in hydrogen transfer which were optimized at the MP2/BS-I level.

genation of methanol with **15a** may occur via transition structure ***anti*-17a** (Figure 5) but the activation energy is 4.2 kcal/mol higher than the reaction via **17a** which has a syn geometry (Figure 2). The resulting hydride complex ***anti*-19a** is less stable than diastereomeric **19a** by 3.5 kcal/mol. In a like manner, formaldehyde is reduced by ***anti*-19a** via the same transition structure ***anti*-17a**. The somewhat higher activation energy, 11.8 vs 7.6 kcal/mol, is ascribable to the use of the equatorial NH proton.

**(g) Origin of Enantioselection in Asymmetric Hydrogen Transfer.** Chiral arene−Ru complexes of type **19** differentiate between enantiofaces of prochiral carbonyl compounds. In a like manner, racemic alcohols can be resolved by chiral 16-electron complexes **15**. The MO calculations suggest that the stereoselectivity in hydrogen transfer originates from the distinction of the two diastereotopic hydrogens on the nitrogen of **19**, $H_{ax}$ and $H_{eq}$, or the two diastereofaces of the nitrogen of **15**. The sense of enantioselection is based primarily on the chirality of the nitrogen-based, five-membered chelate ring in the TS.

Reduction of formaldehyde with **19** occurs via TS **17** utilizing the axially oriented N−$H_{ax}$ linkage and the hydride on Ru (Scheme 4). The reverse dehydrogenation of methanol with **15** proceeds via the same TS **17**. Since **17** is chiral, replacement of formaldehyde by acetaldehyde, or methanol by ethanol, leads to diastereomeric TSs $\mathbf{36_S}$ (more stable) and $\mathbf{36_R}$ (less stable), as illustrated in Figure 2. The $\delta$ chelate ring gives a preference for the *Si* face selection in acetaldehyde reduction and the *pro-S* hydrogen selection in ethanol dehydrogenation by 0.6 kcal/mol. The calculation suggests that the suitable combination of chiral auxiliaries and arene ligands on the Ru center and substituents of the carbonyl substrates can generate a distinct bias for the asymmetric reaction.

**(h) Use of Ethylenediamine as an Auxiliary.** The calculated structures and energies of the Ru complexes possessing ethylenediamine ligands (**b** series) are similar to those derived from ethanolamine (**a** series). The energy profiles are given in Scheme 4, and the detailed three-dimensional structures are illustrated in Figures 1 and 2.

Dehydrogenation of methanol by **15b** by way of **16b** affords **18b** and then free formaldehyde and Ru hydride **19b**. The overall endothermicity, 2.7 (8.8) kcal/mol,[43] is similar to that for the **a** series which is 1.4 (5.7) kcal/mol. The calculated $E_a$ in the step **16b** → **18b**, 24.4 (16.8) kcal/mol, is higher than the value, 19.7 (12.2) kcal/mol, in the **a** series, while reduction of formaldehyde in **18b** occurs with an activation energy of 13.1 (1.5) kcal/mol which is to be compared with 15.8 (4.7) kcal/mol for the **a** series. The TS **17b** is above $CH_3OH$ + **15b** and $CH_2O$ + **19b** by 9.6 and 6.9 kcal/mol, respectively. The MO and DFT calculations give similar but quantitatively somewhat different results.

The structure of the formal 16-electron complex **15b** approximates $C_2$ symmetry. The nonbonding electrons at N are donated to the Ru center. As a consequence, the lengths of the two equivalent Ru−N bonds, 1.899 (av) (1.965) Å,[43] become much shorter than the Ru−$NH_2$ distance in **14b**, 2.124 Å, **19b**, 2.143 (2.198) Å, and **21b**, 2.124 (2.168) Å. The nitrogen atoms are nearly planar, as judged from the sum of the three bond angles, 354° (354.3°). The length of the Ru-amide nitrogen bonds in the 18-electron complexes, 2.037 (**14b**), 2.024 (**19b**), and 2.020 Å (**21b**), are between those of **15b**, 1.899 (av) Å, and normal Ru-amine bonds, 2.12−2.14 Å. Notably, the nitrogen atoms are considerably pyramidized.

The structure of TS **17b** is very similar to **17a** except for the pyramidal structure at the amide nitrogen (Figure 2), suggesting a considerable 18-electron character at the Ru.

### Correlation of the Calculations with Experiments

The calculated reaction pathway strongly contradicts previous perceptions (Scheme 2) but corroborates many of our earlier experimental observations.[10−15]

**(a) Ligand Acceleration.**[54] In situ generated **14** is in fact an excellent precatalyst effecting transfer hydrogenation of acetophenone with 2-propanol containing KOH.[10,11] Although a mixture of $RuCl_2(\eta^6$-benzene) dimer and KOH is almost inactive for the reduction at room temperature, addition of an equimolar amount of ethanolamine or *N*-tosylethylenediamine as ligand enhanced the rate significantly to give 1-phenylethanol. The turnover frequencies, defined as mol of product per mol of Ru per hour, were 227 and 86, respectively. The 16- and 18-electron complexes **15** and **19** or analogues would be involved in the transfer hydrogenation

**(b) Structures of Ru(II) Complexes.** The structural characteristics of the Ru complexes **14**, **15**, and **19** obtained by the MO calculations agree with those of the corresponding isolated complexes. When (1*S*,2*S*)-*N*-tosyl-1,2-diphenylethylenediamine and *p*-cymene were used as ancillaries, the Ru chloride **8** (precatalyst) and hydride **10** (intermediate) having an *R*-configured Ru center were obtained. In accord with the MO prediction, these octahedral complexes have the same $\delta$ five-membered ring as illustrated by the X-ray crystallography.[13]

The presence of the H···Cl hydrogen bond in **14** has been found in the crystallographic structure of **8** (arene = *p*-cymene, $R^1 = R^2 = C_6H_5$). The only discrepancy is the pyramidal configuration of the nitrogen atoms in the calculated structures of the ethylenediamine series (Scheme 4, Y = NH). The real complexes possess a tosyl substituent which makes the nitrogen atoms flat through conjugation. The Ru−amide bond in the square−planar complex **15** is predicted to be very short because

(54) Berrisford, D. J.; Bolm, C.; Sharpless, K. B. *Angew. Chem., Int. Ed. Engl.* **1995**, *34*, 1059.

of the donation of nonbonding electrons of the nitrogen atoms to Ru. This is consistent with the crystallographic structure of **12** (arene = *p*-cymene, $R^1 = R^2 = C_6H_5$).[13]

**(c) Role of Inorganic Bases.** The calculation indicates that a strong base such as KOH is necessary for the generation of the 16-electron catalyst **15** from the 18-electron Ru halide **14** by hydrogen halide elimination via a Dcb mechanism.[55] Since the conversion, **14a** → **15a** + HCl, is calculated to be highly endothermic, $\Delta E = 36.5$ kcal/mol (Table 1), the resulting HCl should be neutralized by a base. Actually, the catalytic activity depends on the quantity of KOH. The in situ generation of the catalyst from $RuCl_2(\eta^6$-arene) and ethanolamine or *N*-tosylethylenediamine in 2-propanol requires 2 mol equiv of KOH;[10,11] one equivalent for ligation of the auxiliary as anion to Ru and the second equivalent for catalyst formation. The base is not utilized for activation of 2-propanol,[7,33] since preformed complexes **10** and **12** (arene = *p*-cymene; $R^1 = R^2 = C_6H_5$) effect smooth hydrogen transfer without additional KOH or other strong bases. Asymmetric transfer hydrogenation of acetophenone in a 0.1 M 2-propanol solution containing **12** (ketone:**12** = 100:1, room temperature) proceeded in the absence or presence of *t*-$C_4H_9OK$ (**12**:base = 1:20) at the same rate and with the same enantioselectivity (*S*:*R* = 98:2).[56]

**(d) Catalytic Cycle and Kinetics.** In the actual catalytic hydrogen transfer reaction, both $\beta$-amino alcohols and *N*-tosylethylenediamine derivatives serve equally as promoters. Most notably, the presence of an $NH_2$ or NH end is crucial for catalytic activity; the $N(CH_3)_2$ analogues are inactive. This is fully consistent with the calculated mechanism in Scheme 4. The possible $\beta$-elimination pathway does not require the primary or secondary amine end.

The calculated mechanism is unique. In most transition metal-based homogeneous catalysis, the bond-forming reaction occurs intramolecularly between metal-coordinated ligands,[57] although sometimes it takes place by a bimolecular mechanism involving a metal complex reagent and an uncoordinated substrate.[58] Bond breaking is normally effected on a metallic center(s). In these processes, the major role of the organic ligands is to perturb the electronic and steric properties of the metallic center. *In contrast, the present redox reaction is characterized by metal−ligand bifunctional catalysis, in which the metal and the surrounding ligand directly participate in the bond-forming and -breaking steps of the dehydrogenative and hydrogenative processes.*[37,52] Primary amines are normally good donors but very weak acids. However, upon interaction with Lewis acidic metals, their acidity and hydrogen-bonding capability are enhanced greatly.[59] This ligation at the same time increases the nucleophilicity of other ligands attached to the metal. Thus, the creation of metal-based 1,4-dipoles with charge alternation provides a powerful guiding principle for inventing new metal−ligand bifunctional catalyses, since many chemical reactions are based on atomic reorganization induced by electronic polarization.

**Scheme 6.** Metal−Ligand Bifunctional Catalysis

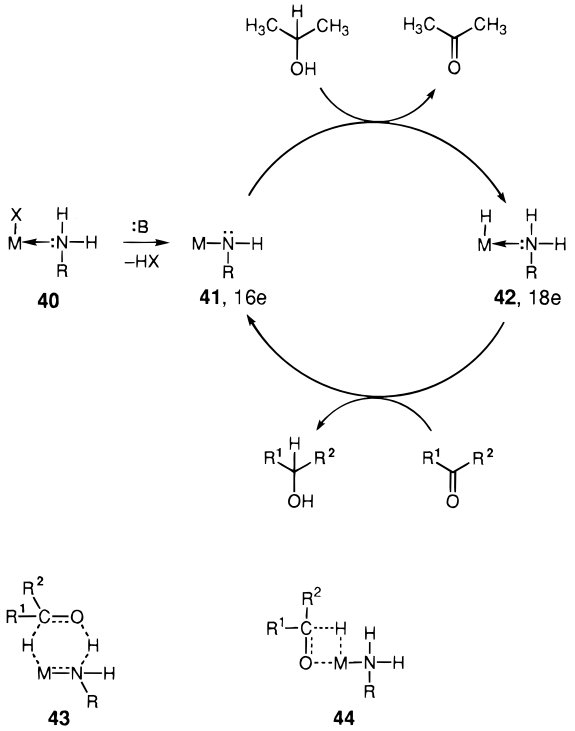


The calculated pathway of hydrogen transfer, $CH_3OH$ + **15** → $CH_2CO$ + **19**, displays a double-well energetic profile involving **16** and **18** (Figure 3), and these hydrogen-bonded intermediates are linked via TS **17**. However, in the actual reaction system in solution, the Ru complexes and organic substrates cannot be free but are strongly stabilized by solvation and other molecular associations. Scheme 6 (M = transition metal, X = anionic ligand; supporting ligands omitted) illustrates the essence of the novel mechanism of transfer hydrogenation of ketones with 2-propanol using **40** as catalyst precursor. This mechanistic model involves only two ground-state components, **41** and **42** in the catalytic cycle. The 16-electron catalyst **41** is actually in a resonance hybrid with the 18-electron species.[47] Most significantly, the amide nitrogen in **41** and the NH proton in **42** play key roles in this metal−ligand bifunctional catalysis. The oxygen atoms of 2-propanol or of the ketonic substrates do not touch the metallic center M in **41** or **42**. Neither metal alkoxide[24] nor carbonyl coordination complex[27] is formed as reactive intermediates throughout the redox reaction. The Ru alkoxide **40** (X = OR), if formed, is nonproductive and reverts back to the catalyst **41** by elimination of the alcohol. Instead, the 2-propanol hydroxy proton interacts with the basic N atom of **41**, while the ketonic oxygen interacts with the acidic NH proton of **42**. Therefore, the ketone reduction does not require any coordinative unsaturation at M, since it occurs in an outer coordination sphere of **42**. The reactive species is a metal hydride (M−H) as has frequently been stated, but hydride delivery to electrophilic carbonyl carbon takes place via a six-membered pericyclic TS **43** rather than by $\pi 2 + \sigma 2$ insertion of the C═O bond into the M−H linkage via **44**. As a result, the product is an alcohol but not a metal alkoxide. The reaction of the amine-coordinated hydride complex **42** and a carbonyl compound affords the metal amide **41** and an alcoholic product via the same TS **43**. In fact, to effect smooth catalytic hydrogen transfer, the presence of an NH function in the auxiliary is crucial.[8d,10−16,17f,g,60] This mechanistic model is different from the currently accepted pathway outlined in Scheme 2.

(55) (a) Tobe, M. L. *Adv. Inorg. Bioinorg. Mech.* **1983**, *2*, 1. (b) Lawrance, G. A. *Adv. Inorg. Chem.* **1989**, *34*, 145.

(56) Yamada, I.; Noyori, R. unpublished.

(57) Collman, J. P.; Hegedus, L. S. *Principles and Applications of Organotransition Metal Chemistry*; University Science Books: Mill Valley, CA, 1987.

(58) For example, see: (a) Klob, H. C.; VanNieuwenhze, M. S.; Sharpless, K. B. *Chem. Rev.* **1994**, *94*, 2483. (b) Jacobsen, E. N. In *Comprehensive Organometallic Chemistry II*; Abel, E. W.; Stone, F. G.; Wilkinson, G. Eds.; Pergamon: New York, 1995; Vol. 12, Chapter 11.1.

(59) (a) Rosenberg, B.; Van Camp, L.; Grimley, E. B.; Thomson, A. J. *J. Biol. Chem.* **1967**, *242*, 1347. (b) Reedijk, J. *Inorg. Chim. Acta*, **1992**, *198−200*, 873.

The possible $\pi 2 + \sigma 2$ reaction between a carbonyl compound and the Ru−H species requires the prior formation of a substrate/Ru $\pi$ complex of type **24** or **24′** which involves a structural change of the arene ligand from $\eta^6$ to $\eta^4$ or even $\eta^2$ (Scheme 3). The efficient carbonyl $\pi$ coordination, particularly with ketones, is difficult for a kinetic reason and also by the presence of a large amount of alcohol possessing a stronger coordination capability. In fact, addition of acetophenone (14-fold excess) to a methanol solution of **8** (arene = *p*-cymene, $R^1 = R^2 = C_6H_5$), an nonreducing analogue of hydride **10**, does not cause any change in the $^1$H NMR spectrum, while the presence of KOH effects smooth transfer hydrogenation under such conditions.[56]

The actual catalytic reaction provides a very rare system in which both the true catalyst and the reactive species have been isolated.[13] In accord with the calculation, the success is attributed to the reversible reactions with different but comparable energetics. In fact, the $\Delta E$ values calculated for the reaction, $CH_3OH$ + **15** → $CH_2CO$ + **19**, are only 1.4 (**a** series) and 2.7 kcal/mol (**b** series) (though 5.7 and 8.8 kcal/mol by B3LYP calculation), suggesting that the equilibrium point can simply be controlled by relative quantities of the hydrogen donor and acceptor. The 16-electron complex **12** (arene = *p*-cymene, $R^1 = R^2 = C_6H_5$) and the 18-electron Ru hydride **10** exhibit equal catalytic activities in transfer hydrogenation between alcohols and carbonyl compounds. A kinetic study of the acetone/2-propanol catalytic cycle firmly eliminated the possibility of turnover-limiting intermediates in the interconversion of **10** and **12**.[13] This fact conforms to the direct mechanism of Scheme 6.

The catalytic behavior of the complexes formed from $RuCl_2$-($\eta^6$-benzene) dimer and $\beta$-amino alcohols with an NH or $NH_2$ end[10,11] is interpreted in the same manner.

**(e) Relative Reactivity of Hydrogen Donors.** The ease with which dehydrogenation occurs varies substantially with the nature of the alcohols. The relative dehydrogenative reactivity obtained by the MO calculation, 2-propanol > ethanol > methanol, is consistent with experimental findings.[13] The calculation suggests that reaction of **15a** and $H_2$ to form **19a** is rather difficult, requiring an activation energy of 25.2 kcal/mol which is significantly higher than those in alcohol dehydrogenations. In fact, **12** (arene = *p*-cymene, $R^1 = R^2 = C_6H_5$) reacts with $H_2$ in toluene at room temperature to give the Ru hydride, but only at 80 atm.[13]

**(f) Chemoselectivity.** The theoretical calculation predicts that the reactivity of unsaturated compounds toward the Ru hydride **19a** depends on the polarity of the double bonds. Carbonyl compounds are reduced to alcoholic products with an activation energy of 16−22 kcal/mol, whereas reduction of methylene imine and ethylene is kinetically more difficult, requiring activation energies of 26.9 and 26.7 kcal/mol, respectively. In addition, bimolecular reaction of ethylene and the Ru hydride is entropically unfavorable. This tendency is consistent with experimental results. Transfer hydrogenation using 2-propanol with **12** (arene = *p*-cymene, $R^1 = R^2 = C_6H_5$) is selective for ketones, leaving olefinic linkages intact.[12] Imines are inactive under the standard conditions using 2-propanol.

**(g) Stability of Alkoxy Ru Complexes.** The only major inconsistency between the calculation and experimental results involves the stability of the Ru alkoxides of type **21**. The calculation predicts that the 16-electron Ru complex undergoes addition of alcohols with a lower activation energy compared to dehydrogenation. The extent of exothermicity, 23.8 (10.8) kcal/mol,[43] of the reaction, **15a** + $CH_3OH$ → **21a**, suggests high stability of the methoxy complex **21a**. Ethanol, 2-propanol, and even *tert*-butyl alcohol are predicted to give the stable alkoxy complexes equally. The calculated stabilities (Table 1) and structures (see Supporting Information) of the alkoxy complexes are similar to **21a**.

Any protic compound can add across the polar Ru−N bond in the formal 16-electron complex to give the corresponding 18-electron complex. This process is reversible. The higher the acidity of the protic compound, the more stable is the adduct, while the neutralization of the acid by a strong base can shift the equilibrium to the 16-electron complex. Experimentally, the isolated purple complex **10** (arene = *p*-cymene, $R^1 = R^2 = C_6H_5$) reacts with HCl or its triethylamine salt and phenol to give the yellowish stable adducts. However, *tert*-butyl alcohol does not change the color or NMR spectrum, however. Addition of an excess amount of 2-propanol, ethanol, or methanol to **10** gives yellow-orange **12** by elimination of a carbonyl compound but no Ru alkoxides are detectable. So far, no experimental evidence for the formation of the alkoxy complexes has been obtained. Thus, the calculated high stabilities of **21a** and other alkoxy complexes are unexpected. Although the entropy difference between the loosely organized **16** and rigid **21** would partly mitigate the actual free-energy difference, there still exists a discrepancy between the theoretical calculations (MO and DFT) and experimental findings. This might be due to the remaining computational error. We consider that in fluid solution addition of alcohols to **12** is occurring reversibly to establish a smooth catalytic cycle. The Ru alkoxides of type **21**, even if formed, are nonproductive but serve as reservoirs of the 16-electron catalyst **12**. Here the close structural resembrance of the alcohol adduct **21** and TS **20** is important to facilitate the alcohol elimination.[61] Otherwise, the catalytic activity of **12** diminishes. In addition, distinct difference in the environments surrounding polar molecules should also be taken into account with respect to the calculation/experiment discrepancy. This is obviously a very difficult problem, however.

**(h) Enantioselection.** The calculated TS structures in Figure 2 help greatly in understanding the origin of enantioselectivity. In actual asymmetric reduction using amino alcohols or diamine derivatives, $NH_2CH(R^2)CH(R^1)YH$ (Y = O or NTs) (Scheme 3), the ligand chirality determines the sense of asymmetric induction, while substitutents on the ligands influence the extent of stereoselectivity. In fact, the chiral complex **12** (arene = *p*-cymene, $R^1 = R^2 = C_6H_5$) modified by (1*S*,2*S*)-*N*-tosyl-1,2-diphenylethylenediamine effects reduction of acetophenone in 2-propanol giving (*S*)-1-phenylethanol in 97% ee.[13] The TS model (*R*)-$\delta$-**45** (Y = NTs) in Figure 6 explains many experimental observations on the asymmetric transfer hydrogenation of prochiral ArCOR (Ar = aryl group, R = alkyl group). The structures, (*R*)-$\delta$-$\mathbf{45_S}$ and (*R*)-$\delta$-$\mathbf{45_R}$, schematically represent diastereomeric TSs differentiating the enantiofaces by an (*R*)-$\delta$-configured Ru hydride. The 1*S*,2*S* configuration of the chiral auxiliary first determines the $\delta$ structure of the five-membered chelate ring, because the bulky phenyl (R′)

(60) For a similar phenomenon in the Ru-catalyzed hydrogenation, see: (a) Ohkuma, T.; Ooka, H.; Hashiguchi, S.; Ikariya, T.; Noyori, R. *J. Am. Chem. Soc.* **1995**, *117*, 2675. (b) Ohkuma, T.; Ooka, H.; Ikariya, T.; Noyori, R. *J. Am. Chem. Soc.* **1995**, *117*, 10417. (c) Ohkuma, T.; Ooka, H.; Yamakawa, M.; Ikariya, T.; Noyori, R. *J. Org. Chem.* **1996** *61*, 4872. (d) Ohkuma, T.; Koizumi, M.; Doucet, H.; Pham, T.; Kozawa, M.; Murata, K.; Katayama, E.; Yokozawa, T.; Ikariya, T.; Noyori, R. *J. Am. Chem. Soc.* **1998**, *120*, 13529. (e) Doucet, H.; Ohkuma, T.; Murata, K.; Yokozawa, T.; Kozawa, M.; Katayama, E.; England, A. F.; Ikariya, T.; Noyori, R. *Angew. Chem., Int. Ed.* **1998**, *37*, 1703.

(61) Moore, J. W.; Pearson, R. G. *Kinetics and Mechanism, 3rd ed.*; Wiley: New York, 1981.

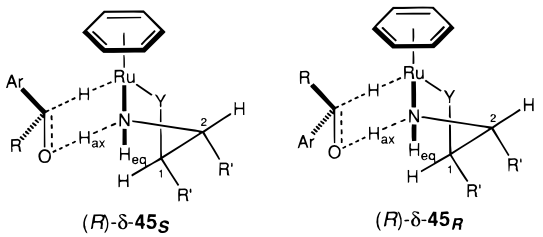


**Figure 6.** Transition structures of asymmetric transfer hydrogenation of aromatic carbonyl compounds.

substituents tend to occupy the equatorial position. This ring geometry is correlated to the *R* absolute stereochemistry of the Ru center for the reason described above. The transfer hydrogenation via (*R*)-*δ*-**45**$_S$ affords (*S*)-ArCH(OH)R, while the diastereomeric structure (*R*)-*δ*-**45**$_R$ leads to (*R*)-ArCH(OH)R. Differentiation between these diastereomeric TSs is actually made by various steric and electronic factors.[10,62] The preference for (*R*)-*δ*-**45**$_S$ over (*R*)-*δ*-**45**$_R$ (Ar = $C_6H_5$, R = $CH_3$, R′ = $C_6H_5$, Y = NTs) is due perhaps to the operation of an attractive CH/*π* interaction[63] between the arene ligand of the complex and the aryl substituent in the substrate.

Because of microscopic reversibility, the didehydro complex **10** (arene = *p*-cymene, $R^1 = R^2 = C_6H_5$) dehydrogenates the *S* alcohol 88 times faster than the R isomer in acetone.[12] This kinetic resolution is understood in terms of the preferred TS (*R*)-*δ*-**45**$_S$ (Ar = $C_6H_5$, R = $CH_3$, R′ = $C_6H_5$, Y = NTs).

1,2-Diphenyl-2-aminoethanol and its *N*-monomethyl derivatives (Y = O) are excellent auxiliaries for in situ generation of chiral Ru catalysts, where the C(1) configuration of the amines is the determinant of the sense of asymmetric induction.[11] The 1*S* stereoisomers consistently give (*S*)-1-phenylethanol regardless the C(2) configuration, either *S* or *R*. As expected from the model (*S*)-*δ*-**45** (Y = O), the phenyl substitutent at C(1) must orient to the equatorial direction in the *δ* five-membered ring, since the axial C(1) substituent induces a serious repulsive interaction with the reacting ketonic substrate. On the other hand, the C(2) substituents are more flexible in terms of the equatorial/axial orientation as can be understood easily from the structure **45**.

## Conclusions

This theoretical study provides new insight for understanding catalytic hydrogen transfer with transition metal complexes possessing primary or secondary amine ligands. The mechanistic model, Scheme 6, is surprisingly simple and different from the currently accepted putative mechanism (Scheme 2). Most significantly, this metal−ligand bifunctional mechanism does not require formation of metal alkoxides or carbonyl−metal coordination complexes in the catalytic cycle. Instead, the hydrogenative transformation of C=O linkages with a coordinatively saturated Ru hydride intermediate and its reverse process occur in an outer coordination sphere of the transition metal with the aid of ligand-substrate hydrogen bonding.[64]

**Acknowledgment.** The authors are grateful to Drs. Shohei Hashiguchi and Karl-Josef Haack of the ERATO Molecular Catalysis Project, Japan Science and Technology Corporation, Professor Takao Ikariya of Tokyo Institute of Technology, and Professor Nobuaki Koga of Nagoya University for their valuable discussions. This work was aided by the Ministry of Education, Science, Sports and Culture of Japan (No. 07CE2004).

**Supporting Information Available:** Cartesian coordinates of **14**−**39** (PDF). This material is available free of charge via the Internet at http://pubs.acs.org.

JA991638H

(62) Corey, E. J.; Helal, C. J. *Tetrahedron Lett*. **1995**, *36*, 9153.

(63) (a) Nishio, M.; Hirota, M. *Tetrahedron* **1989**, *45*, 7201. (b) Nishio, M.; Hirota, M.; Umezawa, Y. *The CH/π Interaction, Evidence, Nature, and Consequences*; Wiley-VCH: New York, 1998.

(64) Very recently, a similar mechanistic conclusion was derived by a Swedish group: Alonso, D. A.; Brandt, P.; Nordin, S. J. M.; Andersson, P. G. *J. Am. Chem. Soc*. **1999**, *121*, 9580.